Available online at www.sciencedirect.com
ScienceDirect
Journal of Sound and Vibration 310 (2008) 442–447
JOURNAL OF SOUND AND VIBRATION
www.elsevier.com/locate/jsvi

Short Communication

Online prediction of the onset of combustion instability based on the computation of damping ratios

Tongxun Yi*, Ephraim J. Gutmark

Department of Aerospace Engineering and Engineering Mechanics, University of Cincinnati, Cincinnati, OH 45220-0070, USA

Received 1 June 2006; received in revised form 27 July 2007; accepted 27 July 2007
Available online 20 September 2007

Abstract

A weighed-least mean square algorithm is used to compute the damping ratios of the linearly stable combustion oscillations, which occur prior to the fully developed nonlinear oscillating stage of combustion instability. The computation of damping ratios is based on the model structure of linear second-order oscillators and the pressure spectrum. Pressure obtained from two experiments on a gas turbine combustion simulator is analyzed. In both cases, the damping ratio drops to the global minimum before combustion oscillations develop into the large-amplitude limit-cycle oscillating stage.

1. Introduction

Modern gas turbines are typically designed to operate in lean premixed or partially premixed mode [1]. Due to equivalence ratio (ϕ) variations and insufficient acoustic damping, combustion instability has become a major technical challenge for dry-low-emission gas turbines. Accurate prediction of the onset and the limiting amplitude of combustion instability is challenging because of the complexities involved in flame/vortex/acoustics interactions, air/fuel mixing, finite chemical kinetics, and the complicated engine geometries. However, for gas turbine operators, even a rough estimation of the safety margin to combustion instability is highly desirable. Towards this goal, Lieuwen [2] has developed a low-order model and a correlation-function-based procedure to ascertain the safety margin to combustion instability using the dynamic pressure data.

This paper computes the damping ratios of the excited acoustic modes using a weighted-least mean square (lms) algorithm. The linearly stable combustion oscillations, which occur prior to the fully developed nonlinear oscillating stage of combustion instability, is modeled as a set of linear, ‘‘closed-loop’’, second-order oscillators, which are forced by the broadband background heat release rate oscillations. Different from Lieuwen's approach, the present method is formulated in the frequency domain, and is applicable to multiple excited modes with unknown frequencies. It is found that the damping ratio drops to the global minimum before the occurrence of combustion instability.

*Corresponding author. Tel.: +1 513 556 1056.
E-mail address: yit@email.uc.edu (T. Yi).

0022-460X/$ - see front matter
doi:10.1016/j.jsv.2007.07.072

Nomenclature

e_i	the scaled broadband background heat release rate oscillations
$f_i(\ldots)$	the deterministic forcing applied to the ith acoustic mode
F_i	the ith frequency point at which the pressure amplitude is computed, Hz
J	the number of frequency points used to compute the damping ratios
N	the sample length
P_0	the mean pressure, Pa
p'	acoustic pressure, Pa
$\hat{p}_{i,j}(\ldots)$	pressure amplitude, Pa
s	the Laplace symbol
$\bar{s}$	the scaled Laplace symbol, $\bar{s} = s/\omega_i$
X	the space vector, m
W	the weight matrix
$\bar{W}_i(\bar{s})$	the scaled transfer function
rms	root mean square
lms	least mean square
ϕ	the equivalence ratio
η_i	the mode coefficient of the ith acoustic mode
ω_i	the "closed-loop" resonant frequency of the ith acoustic mode, rad/s
ς_i	the "closed-loop" damping ratio of the ith acoustic mode

2. Methodology

2.1. Low-order modeling of linearly stable combustion oscillations prior to the onset of combustion instability

Lieuwen [2] has developed a low-order model for analyzing the onset of combustion instability, which is used as a starting point of the present paper. Essentially Lieuwen's model is a linearized version of the nonlinear models developed by Zinn and Culick in the 1970s [3,4] and [2–4]. By Galerkin projection, pressure oscillations within a combustor can be formulated as a set of second-order, coupled, nonlinear oscillators,

$$p'(\vec{X}, t) = p_0 \sum_{i=1}^{\infty} \eta_i(t)\psi_i(\vec{X}). \tag{1}$$

$$\frac{d^2\eta_i}{dt^2} + 2\tilde{\varsigma}_i\tilde{\omega}_i\frac{d\eta_i}{dt} + \tilde{\omega}_i^2\eta_i = f_i\left(\eta_j, \frac{d\eta_j}{dt}, \frac{d\eta_j(t-\tau)}{dt}, \ldots\right) + \tilde{e}_i \quad i,j = 1,\ldots,\infty. \tag{2}$$

where ψ_i, η_i, and $\tilde{\varsigma}_i$ denote the mode shape, the mode coefficient, and the damping ratio of the ith acoustic mode, respectively. $\tilde{e}_i(t)$ refers to the broadband background heat release rate oscillations, which will be explained later. The term of $d\eta_j(t-\tau)/dt$ accounts for the effects of the time delay (τ) and equivalence ratio variations on combustion oscillations, which has not been explicitly included in Refs. [2–4]. The heat release response to flow and acoustic disturbances may involve multiple time delays, and the time delays may also appear in the form of $\eta_j(t-\tau)$. Without loss of generality, we only consider the velocity-coupling mechanism, i.e. the term of $d\eta_j(t-\tau)/dt$. If the term of $\eta_j(t-\tau)$ is included in $f_i(\ldots)$, similar analysis can be applied. Since the present paper is mainly concerned with the linearly stable small-amplitude combustion oscillations, $f_i(\ldots)$ is linearized into functions of η_j, $d\eta_j/dt$, and $d\eta_j(t-\tau)/dt$ [2]. This results in the following equations:

$$\frac{d^2\eta_i}{dt^2} + 2\hat{\varsigma}_i\hat{\omega}_i\frac{d\eta_i}{dt} + \hat{\omega}_i^2\eta_i = \tilde{e}_i + \varepsilon_i\dot{\eta}_i(t-\tau) \quad i = 1,\ldots,\infty. \tag{3}$$

Note that $\varepsilon_i = \partial f_i/\partial\dot{\eta}_i(t-\tau)$. In Eq. (3), the possible linear coupling between acoustic modes is neglected.

We first consider a small time delay that allows the following approximation to hold:

$$\dot{\eta}_i(t-\tau) \approx \dot{\eta}_i(t) - \ddot{\eta}_i(t)\tau. \tag{4}$$

By plugging Eq. (4) into Eq. (3), one gets

$$\frac{d^2\eta_i}{dt^2} + 2\varsigma_i\omega_i\frac{d\eta_i}{dt} + \omega_i^2\eta_i = e_i \quad i = 1,\ldots,\infty. \tag{5}$$

Here $2\varsigma_i\omega_i = (2\hat{\varsigma}_i\hat{\omega}_i - \varepsilon_i)/(1+\varepsilon_i\tau)$, $\omega_i^2 = \hat{\omega}_i^2/(1+\varepsilon_i\tau)$, and $e_i = \tilde{e}_i/(1+\varepsilon_i\tau)$. One can infer from Eq. (5) that, for the time delay satisfying Eq. (4), an increase in τ decreases the damping ratio. Note that the approximation of Eq. (4) is not applicable for large time delays, say up to several pressure cycles. To simplify the analysis, we assume that the pressure oscillating amplitude and frequency change slowly, which is usually a reasonable assumption for a linear oscillator with a very small damping ratio. For certain time delays, such as $\hat{\tau} = (2\pi n)/\omega_i \quad (n = 1, 2, \ldots)$, one can approximate that $\dot{\eta}_i(t-\hat{\tau}) \approx \dot{\eta}_i(t)$, which allows Eq. (3) to be written as

$$\frac{\mathrm{d}^2\eta_i}{\mathrm{d}t^2} + (2\hat{\varsigma}_i\hat{\omega}_i - \varepsilon_i)\frac{\mathrm{d}\eta_i}{\mathrm{d}t} + \hat{\omega}_i^2\eta_i = \tilde{e}_i \quad i = 1, \ldots, \infty. \tag{6}$$

Obviously the damping ratio decreases for $\varepsilon_i > 0$ and increases for $\varepsilon_i < 0$. On the contrary, in the case of $\hat{\tau} = (2\pi(n-0.5))/\omega_i \quad (n = 1, 2, \ldots)$, the damping ratio increases for $\varepsilon_i > 0$ and decreases for $\varepsilon_i < 0$. Stability analysis for τ with a general value is not very straightforward. Here we simply assume that the closed-loop damping ratio ς_i has incorporated the effects of the time delay.

$\tilde{e}_i(t)$ in Eq. (3) is interpreted as the broadband background heat release oscillations caused by the wideband turbulence. It is worthwhile to point out that the deterministic heat release rate oscillations causing flame/acoustics/vortex interactions have been assimilated into the stiff and damping terms in Eq. (5), so $\tilde{e}_i(t)$ only contains the background heat release rate oscillations. Since the hydrodynamic instability is amplified over much wider frequency ranges than the acoustic modes [5,6], $\tilde{e}_i(t)$ is assumed to have constant amplitude within a small region around the acoustic resonant frequency.

2.2. Determination of the damping ratios

Taking Laplace transformation of Eq. (5), one gets

$$W_i(s) = \frac{\eta_i(s)}{E_i(s)} = \frac{1}{s^2 + 2\varsigma_i\omega_i s + \omega_i^2}. \tag{7}$$

Since $e_i(t)$ has constant amplitude within a small region around the resonant frequency, the pressure amplitude around ω_i can be expressed as

$$\hat{P}_{i,j}(\bar{\omega}_{i,j}) = \beta_i \Big/ \sqrt{(1-\bar{\omega}_{i,j}^2)^2 + 4\varsigma_i^2\bar{\omega}_{i,j}^2} \quad (\hat{P}_{i,j} = p_0\eta_{i,j}\omega_i^2; \beta_i = p_0 E_i(s); \quad j = 1, 2, \ldots, J). \tag{8}$$

Here $\bar{\omega}_{i,j}$ refers to the normalized frequency, $\bar{\omega}_{i,j} = 2\pi F_j/\omega_i$. $F_j (j = 1,2, \ldots, J)$ denotes the frequency points nearby the resonant frequency ω_i. β_i can be perceived as the normalized amplitude of the background heat release rate oscillations. Theoretically, for each acoustic resonant mode, ς_i and β_i can be uniquely determined from two frequency points nearby the resonant frequency in the pressure spectrum. However, the pressure spectrum usually exhibits non-physical irregular peaks around the resonant frequencies. For the accuracy to be improved, a weighted-lms algorithm is used in this paper.

Assume that J points nearby the resonant frequency ω_i are used for damping ratio computations. For each frequency point, one can write down

$$\beta_i^2 - 4\varsigma_i^2\bar{\omega}_{i,j}^2\hat{P}_{i,j}^2 = (1-\bar{\omega}_{i,j}^2)^2\hat{P}_{i,j}^2 \quad (j = 1, 2, \ldots, J). \tag{9}$$

Here we suggest $J > 10$, so the problem is overly determined. We use a weighted-lms algorithm to compute the damping ratio

$$\begin{pmatrix} \beta_i^2 \\ \varsigma_i^2 \end{pmatrix} = (C^{\mathrm{T}}WC)^{-1}C^{\mathrm{T}}WB. \tag{10}$$

Here,

$$C = \begin{pmatrix} 1 & -4\bar{\omega}_{i,1}^2 \\ 1 & -4\bar{\omega}_{i,2}^2 \\ \cdots & \cdots \\ 1 & -4\bar{\omega}_{i,J}^2 \end{pmatrix} \quad \text{and} \quad B = \begin{pmatrix} (1-\bar{\omega}_{i,1}^2)^2 \hat{P}_{i,1}^2 \\ (1-\bar{\omega}_{i,2}^2)^2 \hat{P}_{i,2}^2 \\ \cdots \\ (1-\bar{\omega}_{i,J}^2)^2 \hat{P}_{i,J}^2 \end{pmatrix}.$$

W is the diagonal weight matrix. The weighted-lms algorithm requires the pressure spectrum. The fast Fourier transform (FFT) algorithm is typically used in offline signal processing to calculate the discrete Fourier transform (DFT). The authors have found difficulties in using this approach for real-time high-accuracy computation, and have developed a modified algorithm for calculating the DFT. Details of this algorithm can be found in Ref. [7].

In the present paper, damping ratio computations are formulated in the frequency domain, while Lieuwen's method is formulated in the time domain. Essentially these two approaches are equivalent. The frequency-domain analysis allows the excited acoustic modes to separate in the pressure spectrum, which is advantageous in the case of multiple excited modes with unknown and time-varying frequencies.

3. Results

Pressure measured from a partially premixed, turpentine-fueled, atmospheric gas turbine combustor is analyzed here. The combustion rig is described in Ref. [8]. The unstable acoustic mode roughly corresponds to the quarter wave mode of the combustion chamber, with a pressure anti-node nearby the dump plane. For the first experiment, combustion occurs in a 0.45-m-long combustion chamber with the fuel split ratio of 0.8, the preheat temperature of 473 K, and the air mass flow rate of 55.6 g/s. The fuel split ratio refers to the ratio of the main fuel flow rate to the total one. Pressure is measured at the chamber exit, 0.2 m away from its center, using a K&J microphone with a sensitivity of 10 mV/Pa. For the second experiment, combustion occurs in a 0.66-m-long combustion chamber with the fuel split ratio of 0, the preheat temperature of 373 K, and the air mass flow rate of 55.6 g/s. Pressure is measured at 0.08 m above the dump plane, using a Kistler pressure transducer with a sensitivity of 10 kPa/V. The first experiment shows combustion instability preceding the lean blowout, with the second one well above the lean blowout. In both experiments, the sampling frequency is 5 kHz, and the sample length is 10,000. The frequency interval for pressure spectrum estimation is 5 Hz.

Fig. 1 compares two pressure spectra, with one computed using the procedures in Ref. [7] and the other using the weighted-lms algorithm. The original pressure spectrum exhibits multiple irregular peaks around the

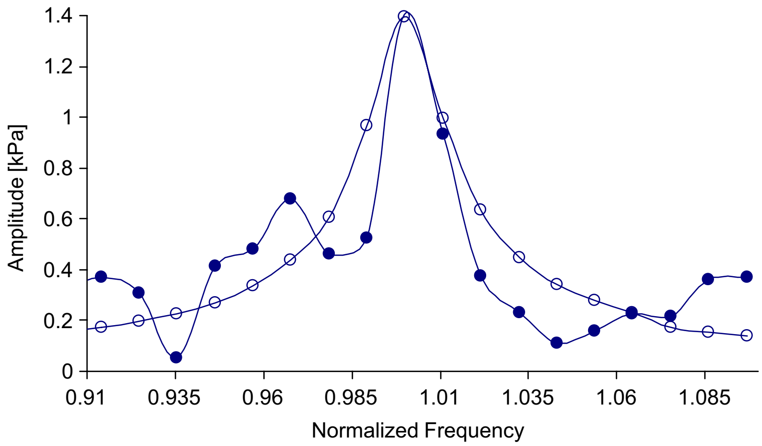

Fig. 1. The original pressure spectrum and the curve-fitted one at $\phi = 0.62$ during the first experiment. ○ Curve-fitted spectrum; ● original spectrum.

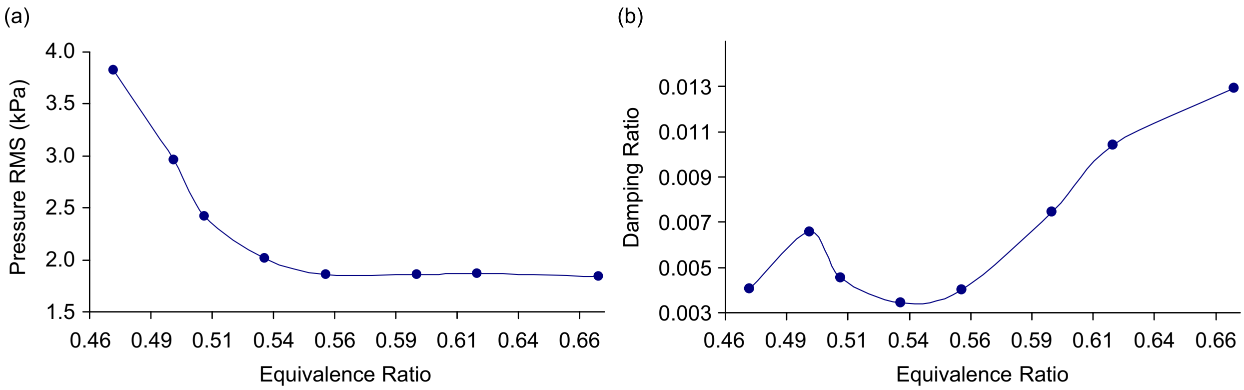

Fig. 2. (a) Pressure rms for the first experiment. (b) Damping ratios for the first experiment.

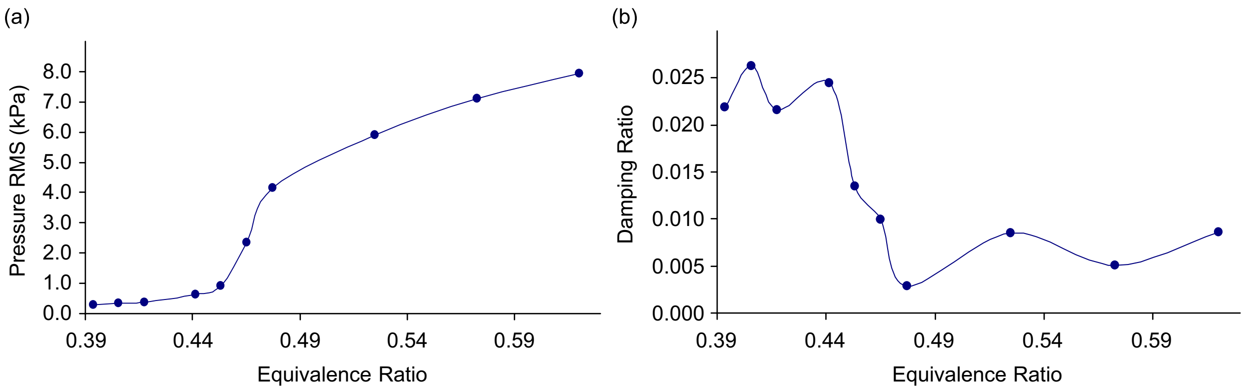

Fig. 3. (a) Pressure rms for the second experiment. (b) Damping ratios for the second experiment.

resonant frequency, which is an intrinsic feature of DFT and FFT. The curve-fitted spectrum is much smoother than the original one, and has the same structure as a second-order linear oscillator. Fig. 2 shows the pressure root mean square (rms) and the damping ratios for the first experiment. Pressure rms is computed from the filtered pressure using a fourth-order Butterworth bandpass filter within [350–450] Hz. One can see that when ϕ is reduced from 0.67 to 0.53, ς_i decreases more than three times, while the pressure rms increases less than 10%. This suggests that the damping ratio is a sensitive index for predicting the safety margin to combustion instability. Note that the procedures described in this paper may not be applied for $\phi < 0.53$ where pressure oscillations are pretty strong. Fig. 3 shows the pressure rms and the damping ratios for the second experiment. Pressure rms is computed from the filtered pressure using a fourth-order Butterworth bandpass filter within [220–300] Hz. By increasing ϕ from 0.44 to 0.48, ς_i decreases more than eight times while the pressure rms increases about six times. Again the procedures described in this paper may not be valid for $\phi > 0.48$ where the pressure oscillating intensity is quite strong.

The accuracy of damping ratio computations is affected by the weight matrix W, the number of frequency points used for curve fitting, and the pressure spectrum. In the above computations, 19 frequency points around the resonant frequency is used for curve fitting, with the diagonal elements of the weight matrix as $[1, 1, 1, 1, 1, 2, 2, 5, 20, 100, 20, 5, 2, 2, 1, 1, 1, 1, 1]$. Larger weights are imposed for frequencies points nearby the resonant frequency because the dominant mode generates non-physical peaks at other frequencies. It is found that a smaller number of frequency points than 19, say 11, can also generate good results. The accuracy of the pressure spectrum can be significantly improved by increasing the sample length. For the procedures described in Ref. [8], the computational complexity within each sample interval is fixed. This allows the pressure spectrum to be accurately determined without sacrificing the real-time performance.

Note that, in the above two experiments, combustion instability is approached by varying the equivalence ratio. Onset of combustion instability may also occur with variations in several other parameters, such as the preheat temperature, the nozzle inlet velocity, or the combustor length. The underlying mechanism responsible for the onset of combustion instability may be different with different control parameters. However, no matter what the control parameter is, the onset of combustion instability is associated with the reduction in the damping ratio.

4. Conclusion

The present paper is concerned with the linearly stable combustion oscillations, which occur prior to the fully developed nonlinear oscillating stage of combustion instability. Stable combustion oscillations are modeled as a set of linear, second-order, closed-loop oscillators, with the broadband background heat release rate oscillations as the input signal. The deterministic heat release oscillations caused by flame/acoustics/vortex interactions have been assimilated into the stiff and damping terms of the low-order models. The damping ratios are determined from the pressure spectrum using a weighted-lms algorithm. Pressure measured from two experiments on a gas turbine combustion simulator is analyzed. It is found that the damping ratio drops to the global minimum before combustion oscillations develop into the nonlinear limit-cycle oscillating stage. The trend of damping ratio variations is consistent with the observations made by Lieuwen in Ref. [2].

References

[1] A.H. Lefebvre, The role of fuel preparation in low-emission combustion, *ASME Journal of Engineering for Gas Turbines and Power* 117 (1995) 617–665.

[2] T. Lieuwen, Online combustor stability margin assessment using dynamic pressure data, *ASME Journal of Engineering for Gas Turbines and Power* 127 (2005) 478–482.

[3] B.T. Zinn, E.A. Powell, Nonlinear combustion instabilities in liquid propellant rocket engines, *Proceedings of the Combustion Institute (International)* 13 (1970) 491–502.

[4] F.E.C. Culick, Nonlinear growth and limiting amplitude of acoustic oscillations in combustion chambers, *Combustion Science and Technology* 3 (1971) 1–16.

[5] T. Poinsot, D. Veynante, *Theoretical and Numerical Combustion*, Edwards Publications, Philadelphia, 2005, p. 423.

[6] C.-M. Ho, P. Huerre, Perturbed free shear layers, *Annual Review of Fluid Mechanics* 16 (1984) 365–424.

[7] T. Yi, E. J. Gutmark, Adaptive control of combustion instability based on dominant acoustic modes reconstruction, *Proceedings of the 44th AIAA Aerospace Sciences Meeting and Exhibit*, Reno, Nevada, 2006, Paper No. AIAA-2006-751.

[8] T. Yi, E.J. Gutmark, Combustion instabilities and control of a multi-swirl atmospheric combustor, *ASME Journal of Engineering for Gas Turbines and Power* 128 (2006) 1–7.